The influence of zooplankton and oxygen on the particulate organic carbon flux in the Benguela Upwelling System

Luisa Chiara Meiritz [1,4], Tim Rixen [1,2], Anja Karin van der Plas[3], Tarron Lamont [5,6,7], Niko Lahajnar [1]

[1] Universität Hamburg, Institute of Geology, Hamburg, Germany
[2] ZMT Leibniz-Centre for Tropical Marine Research, Bremen, Germany
[3] NatMIRC Ministry of Fisheries and Marine Resources, Swakopmund, Namibia
[4] GEOMAR Helmholtz Center for Ocean Research, Kiel, Germany
[5] Oceans & Coasts Research, Department of Forestry, Fisheries, and the Environment, Cape Town, South Africa
[6] Bayworld Centre for Research & Education, Cape Town, South Africa
[7] Oceanography Department, University of Cape Town, Cape Town, South Africa

Correspondence to: Luisa Chiara Meiritz (lmeiritz@geomar.de/ luisa-c-meiritz@web.de)

Abstract. We conducted sediment trap experiments in the Benguela Upwelling System (BUS) in the south-eastern Atlantic Ocean to study the influence of zooplankton on the flux of particulate organic carbon (POC) through the water column and its sedimentation. Two long-term moored and sixteen short term free-floating sediment trap systems (drifter systems) were deployed. The mooring experiments were conducted over more than a decade (2009-2022) and the sixteen drifters were deployed on three different research cruises between 2019 and 2021. Zooplankton was separated from the trapped material and divided into 8 different zooplankton groups. In contrast to zooplankton which actively carries POC into the traps in the form of biomass (active POC flux), the remaining fraction of the trapped material was assumed to fall passively into the traps along with sinking particles (passive POC flux). Our results show, in line with other studies, that copepods dominate the active POC flux, with the active POC flux in the southern BUS (sBUS) being about three times higher than in the northern BUS (nBUS). In contrast, the differences between the passive POC fluxes in the nBUS and sBUS were small. Despite large variations, which reflected the variability within the two subsystems, the mean passive POC fluxes from the drifters and the moored traps could be described using a common POC flux attenuation equation. However, the almost equal passive POC flux, on the one hand, and the high POC concentration in the surface sediments of the nBUS in comparison to the sBUS, on the other hand, imply that the intensity of the near-bottom oxygen minimum zone (OMZ), which is more pronounced in the nBUS than in the sBUS, controls the preservation of POC in sediments significantly. This highlights the contrasting effects of the globally observed expansion of OMZs, which on the one hand mitigates the accumulation of CO_2 in the atmosphere and the ocean by increasing POC storage in sediments and on the other hand poses a threat to established ecosystems and fisheries.

Introduction

Carbon storage by pelagic marine ecosystems, known as the biological carbon pump, exerts a strong control over atmospheric CO_2 concentrations by influencing CO_2 storage in the ocean and underlying sediments. Although scientific studies have widely shown that the biological pump responds to climate change (e.g., Devries and Deutsch, 2014; Duce et al., 2008; Laufkötter et al., 2017; Riebesell et al., 2007) and is affected by fisheries (Bianchi et al., 2021), it is not yet possible to predict the extent and the signs of changes (Laufkötter and Gruber, 2018;

Passow and Carlson, 2012; Rixen et al., 2024). These uncertainties reduce confidence in climate predictions (Passow and Carlson, 2012), call into question sustainability criteria related to the growing blue economy (Jouffray et al., 2020) and assessments of the state of the ocean such as the Ocean Health Index (Halpern et al., 2012). In addition, pelagic ecosystems, which fuel the biological carbon pump and enable the transfer of POC to the sediment, are not considered as blue carbon ecosystems (e.g. Lovelock and Duarte, 2019; Macreadie et al., 2019), which means that their response to human perturbation is largely ignored in national reports to the UNFCC (United Nations Framework Convention on Climate Change) in the framework of the Paris Agreement. As shelves located in the 200-mile exclusive economic zone (EEZ) are of great relevance for the global carbon cycle (Rixen et al., 2024), lately efforts are being made to include sediments in the blue carbon concept (European Marine Board, 2023; von Maltitz et al., 2024). To emphasize the relevance of this effort, it should be noted that the carbon storage in the EEZs with 1092 - 1166 Pg C (Atwood et al., 2020) by far exceed those in the classic blue carbon ecosystems (salt marshes, mangroves and seagrasses: ~7.3 - 22.7 Pg C (Pendleton et al., 2012).

One of the difficulties in studying pelagic ecosystems is that they evolve in a moving medium, the ocean. The residence time of ocean water on the shelf is on average around 12 to 17 months (Lacroix et al., 2021), so that it falls only temporarily under the jurisdiction of an individual state. Nevertheless, they have a long-term impact on carbon storage in territorial waters through their influence on carbon sedimentation. Although processes that control the delivery of POC to the sediment are known in general, there are also a number of unknown and difficult to determine processes as well as methodological problems in determining POC fluxes to the sediment. As a result, global estimates of the amount of POC exported from the sunlit surface ocean (export production) vary between 1.8 - 27.5 10^{15} g C yr^{-1} (Del Giorgio and Duarte, 2002; Honjo et al., 2008; Lutz et al., 2007).

The delivery of POC to the sediment begins with primary production, which converts dissolved inorganic carbon into POC. Incorporated into particles and following gravity, these particles sink through the water column onto the sediment. Three different types of particles are generally distinguished, namely faecal pellets from zooplankton and fish, amorphous aggregates (marine snow) and remains of dead marine organisms (Turner, 2015). Global modelling studies conclude that faecal pellets are on average responsible for 16 - 85 % of gravitational POC export (Archibald et al., 2019; Nowicki et al., 2022), which is consistent with sediment trap results. In sediment trap samples, the proportion of faecal pellets in the POC can vary between 1 and 100 %, but is often around 40 %. (Turner, 2015).

On their way through the water column, bacteria and zooplankton degrade the sinking organic material. The decrease in sinking POC with depth has been described by a whole series of relatively simple attenuation equations, of which the so-called Martin equation is probably the best known (Martin et al., 1987). The Martin equation (Eq. 1) is based on the POC flux at the base of the mixed layer (F_{MLD}), the water depth (z), the mixed layer depth (MLD), and the attenuation rate (b).

$$F_z = F_{MLD} * (\frac{z}{MLD})^b \tag{1}$$

The POC flux at the base of the MLD corresponds to the export production which, like all other parameters, can vary spatially and temporally (Martin et al., 1987 and e.g. Giering et al. 2014). A comparison of some of these equations shows that they all represent the measured data well but differ significantly in their implications, e.g., with regard to the calculation of the POC degradation rates inherent in them (Cael and Bisson, 2018). In addition, these equations have also been criticized because they do not consider the role of zooplankton. The diurnal vertical migration of zooplankton is one of the largest known mass movements in the animal kingdom, extending from the surface to water depths of 200 to 650 m (Bianchi et al., 2013). However, model calculations show that zooplankton

degrade approximately 15 % and 43 % of the exported POC (Bianchi et al., 2013; Archibald et al., 2019). On average, this would be around 30 %, which is consistent with the results of a comprehensive field study from Giering et al. (2014) in the Atlantic Ocean. This study found that 70 - 92 % of the sinking POC at depths between 100 and 1000 m was degraded by bacteria, which conversely means that up to 30 % of the POC is decomposed by zooplankton (Giering et al., 2014). To investigate the influence of zooplankton on POC flux and sedimentation, we conducted sediment trap experiments in the BUS, where the accumulation of POC in the sediment can become so high that in some places 'mud belts' are formed, characterized by POC concentrations >12 % and high POC storage in the sediments (Fig. 1, van der Plas et al., 2007; Monteiro et al., 2005; Emeis et al., 2018; Atwood et al., 2020).
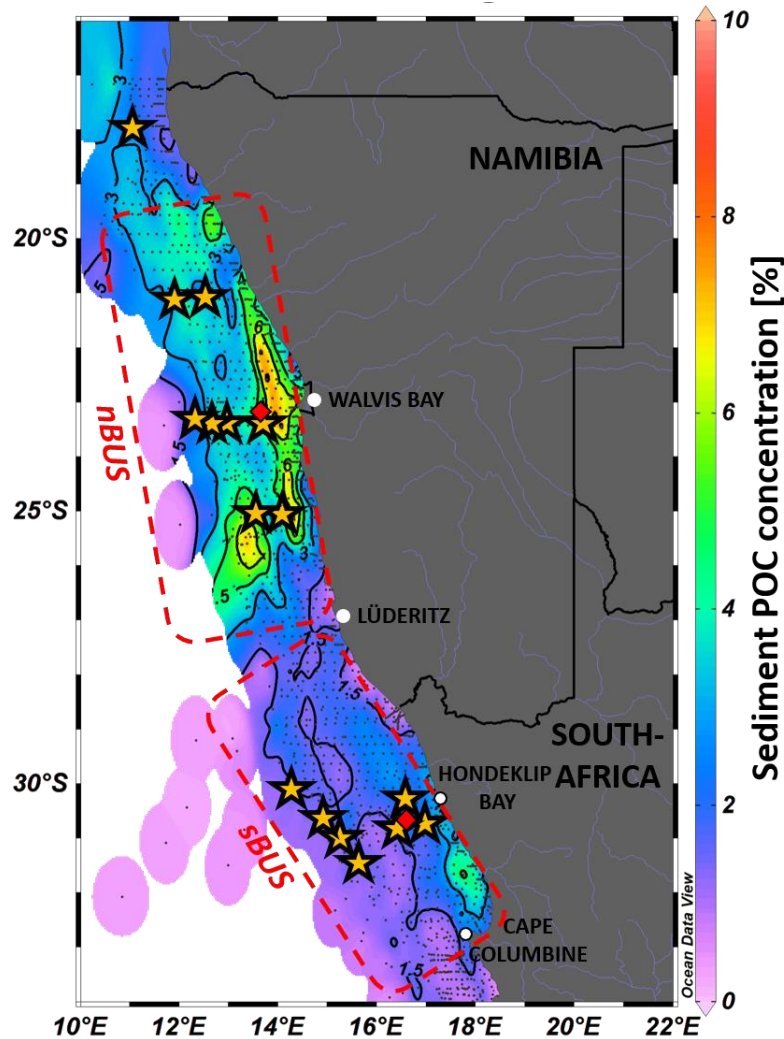

Figure 1 POC concentration of surface sediment samples in the BUS from various research expeditions published in Emeis et al. (2018). Yellow stars show deployment drifter positions; red diamonds show long-term mooring locations. Contour lines in 1.5 % steps. Red dashed areas indicate the nBUS and sBUS, respectively (Hutchings et al., 2009).

Working area

The BUS is one of the four major Eastern Boundary Upwelling Systems, which are among the most productive marine ecosystems in the world's ocean (Chavez and Messié, 2009; Carr, 2001). Although they cover only 2 % of the global ocean surface, they provide more than 20 % of the total global marine fishery yields (Pauly and Christensen, 1995; Sydeman et al., 2014) and contribute about 11 % to the global export production (Chavez and

100   Toggweiler, 1995). In almost all Eastern Boundary Upwelling Systems, distinct OMZs have been formed below the euphotic zone at depths between approximately 100 and 1000 m (e.g. Monteiro et al., 2011). They are the product of high oxygen consumption, caused by the degradation of the exported POC, compared to the ventilation of the OMZ (Rixen et al., 2020 and references therein). Their expansion due to global warming is considered one of the greatest threats to marine life (Stramma et al., 2008; Stramma et al., 2012), alongside global warming and

105   ocean acidification (https://www.globalgoals.org/goals/14-life-below-water/).

The BUS extends approx. from the Kunene river (~17°S) in the north to Cape Agulhas (~35°S) in the south. It is driven by the southeast trade winds that result from the pressure difference between the South Atlantic high and the continental low over southern Africa, which leads to the formation of individual, particularly prominent upwelling cells along the shoreline (e.g. Kämpf and Chapman, 2016; Sell et al., 2024; Shannon and Nelson, 1996;

110   Veitch et al., 2009). The strongest is the Lüderitz Cell, which divides the BUS at about 27°S into a northern (nBUS) and a southern subsystem (sBUS) (Hutchings et al., 2009; Shannon and O'tool, 2003). The two subsystems are influenced by two different source water masses, namely the South Atlantic Central Water (SACW) in the north and the Eastern South Atlantic Central Water (ESACW) in the south (McCartney, 1977; Shillington et al., 2006) which differ in their biogeochemical properties (Mohrholz et al., 2008; Flohr et al., 2014). Compared to the

115   ESACW, the SACW is low in oxygen and enriched in dissolved nutrients, which distinguishes the OMZs in the two subsystems from each other. In the nBUS, the OMZ is essentially controlled by the seasonally variable inflow of the oxygen-poor SACW (Monteiro et al., 2006; Mohrholz et al., 2008), whereas the sBUS OMZ is assumed to be influenced to a much greater extent by the seasonally varying productivity and the resulting export production (Bailey, 1991; Pitcher and Probyn, 2011; Pitcher et al., 2014; Lamont et al., 2015). The consequences are that the

120   sBUS OMZ develops predominantly in the bottom waters on the shelf while the nBUS OMZ also extends along the continental slope (Fig. 2). Although occasional mass mortality events of, e.g. rock lobsters, indicate that anoxic conditions occur in the shelf region (Cockcroft, 2001; Cockcroft et al., 2008; Hutchings et al., 2009), the oxygen concentrations in the sBUS OMZ are generally higher than in the nBUS OMZ. Accordingly, anoxic processes such as anammox and denitrification have a significant effect on the nitrogen cycle in the nBUS (Kalvelage et al.,

125   2011; Nagel et al., 2013), and anoxic events, during which reduced gases such as CH_4 and H_2S are released from the sediment, often occur in association with an increased influx of SACW in summer (Ohde and Dadou, 2018; Ohde et al., 2007).

(a) nBUS Transect 21°S

(b) sBUS Transect 32°S
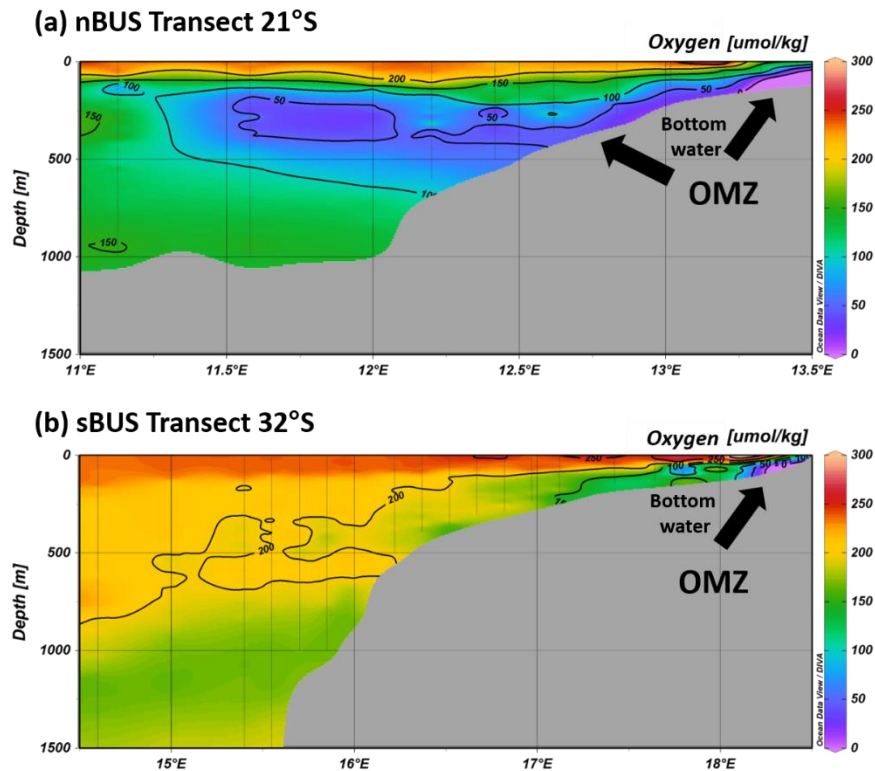
Figure 2 Oxygen concentrations along a transect in the nBUS and sBUS during cruise SO285, showing the near-bottom OMZ
in the nBUS (a) and sBUS (b), and the OMZ on the continental slope in the nBUS. Oxygen data (unpublished) from CTD casts
conducted during cruise SO285.

Calculations of the upwelling velocities from wind fields in comparison with model results show that strong spatial variations occur within the two subsystems due to the interaction of wind stress and the geometry of the coast. Strong upwelling events at the coast can e.g., be accompanied by a weak upwelling in the adjacent ocean (Bordbar et al., 2021). In addition, mesoscale and sub-mesoscale processes such as eddies, filaments, the formation of oceanic fronts and vertical mixing influence the vertical water mass transport and with it the wind driven upwelling (Rixen et al., 2021b; Flynn et al., 2020; Bakun, 2017; Rubio et al., 2009). As a result, localised upwelling can exhibit a pronounced seasonality, such as off Walvis Bay in the nBUS, while the seasonality in other regions of the two subsystems is only weakly pronounced (Bordbar et al., 2021).

In contrast, sea surface temperatures (SST) in both subsystems show a pronounced seasonality with lower temperatures in winter and higher temperatures in summer (Fig. 3). Off Cape Columbine in the sBUS, winter cooling is accompanied by weaker upwelling while off Walvis Bay in the nBUS, stronger upwelling develops in phase with winter cooling whereas summer heating is associated with weaker upwelling (Bordbar et al., 2021).
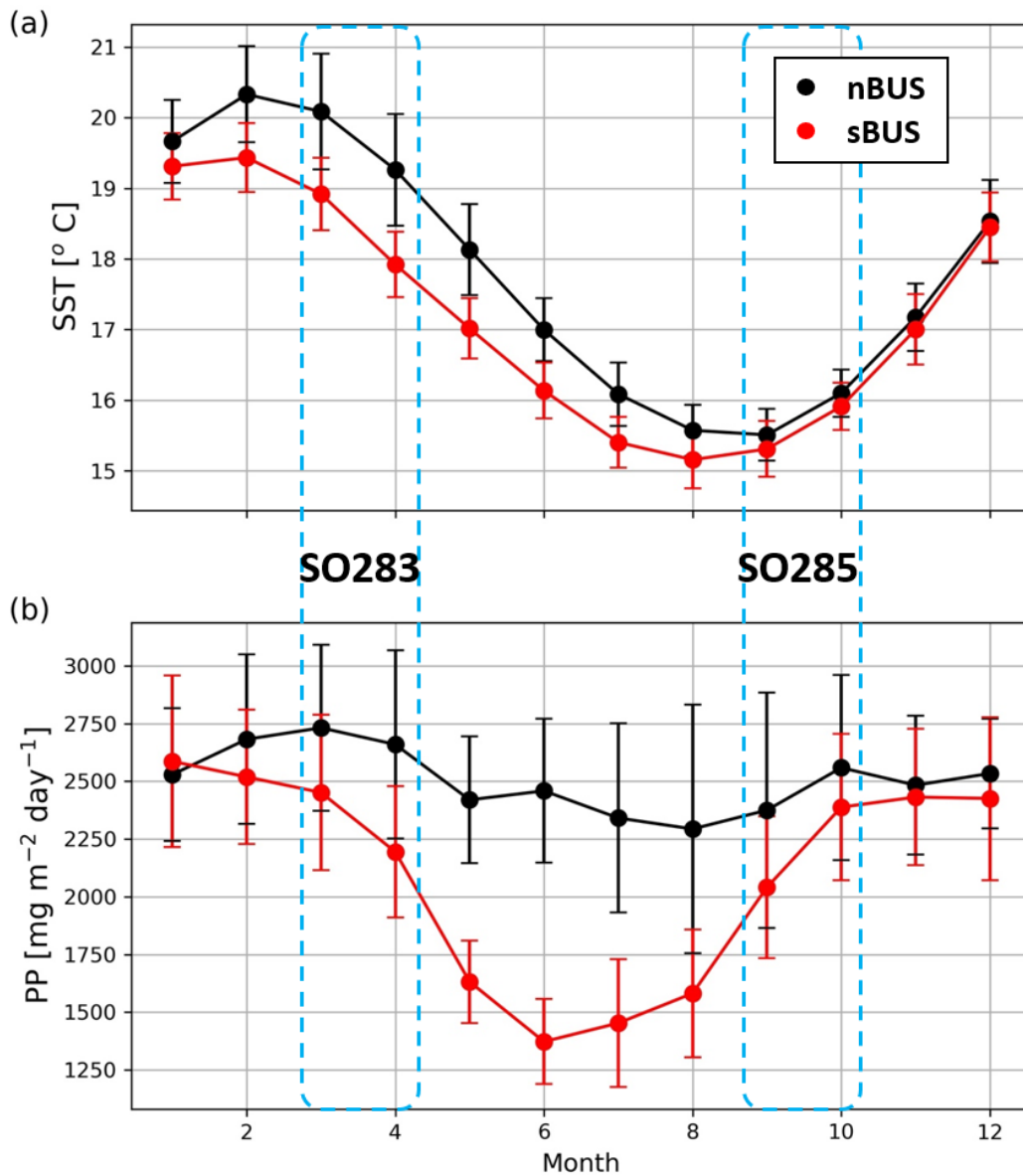
Figure 3 Monthly mean annual cycles of sea surface temperatures (SST, a) and primary production rates (PP, b) in the nBUS and sBUS area, respectively. Satellite data (OI SST, and PP) have been downloaded in November 2023 (see method section). Dotted areas indicate the sampling periods of SO283 and SO285 cruises, respectively. Error bars indicate the standard deviation of PP and SST within the time period 1981-2023.

These results agree with observations along the Namibian monitoring line off Walvis Bay (23°S, Louw et al., 2016). They showed that, favoured by the weak upwelling and summer warming, a relatively strong stratification develops in the surface water at the beginning of the summer which dissipates at the end of the summer with the onset of winter cooling and the strengthening of the upwelling (Louw et al., 2016). Highest concentrations of chlorophyll were found in transitional phases, with clear maxima at the beginning and end of the summer between November and January, and March and April, respectively (Louw et al. 2016).

Averaged over the two subsystems, the primary production derived from satellite data (see Fig. 3) follows the seasonal pattern of chlorophyll concentration off Walvis Bay in both subsystems in so far as that primary production is lower on average in winter than in summer (average over 1981-2023). In the sBUS, however, the seasonality is much more pronounced than in the nBUS, which, as already mentioned, also affects the seasonality of the sBUS OMZ.

Methods

We deployed two long-term sediment trap systems to investigate the seasonality and the influence of zooplankton on the POC, one off Walvis Bay in the nBUS and one off Hondeklip Bay in the sBUS. In parallel, a total of 16 free-floating sediment trap arrays (drifters) were deployed on three research cruises (Table 3, Fig. 1). The moorings were equipped with Hydro-Bios MST 12 traps and for the drifter systems, Hydro-Bios Saarso single traps were used. Both trap versions have an identical cylinder design with a collection area of 0.015 m². The openings of the traps are fitted with a 2x2 cm honeycomb mesh to prevent macroparticles from entering and clogging the trap. The long-term moorings are part of ongoing long-term sediment trap studies in the BUS, considering for this study a mooring period between April 2010 and August 2022 off Walvis Bay for the nBUS (Rixen et al., 2021b; Vorrath et al., 2018) and between October 2019 and April 2022 in Hondeklip Bay for the sBUS (Rixen et al, 2021a) (Table 2, Fig. 6a). Both sites are located close to the coast line in water depths between 100 and 200 m. Hydro-Bios MST-12 sediment traps were moored at both stations in trap depths of approximately 64 and 100 m, respectively. The traps were equipped with twelve sample bottles (250 ml Nalgene) that rotated under the trap at fixed programmed intervals. The collection intervals of the individual sample bottles were between 9 and 40 days. The 16 drifters were deployed during the cruises with the German RVs Meteor (M153) and Sonne (SO283, SO285, Rixen et al., 2021b; Lahajnar et al., 2021). During the cruises a total of 83 single sediment traps were deployed along with the drifter arrays (Table 1). To keep the drifter in an upright position, they were equipped with a buoyancy unit at the upper end and a 30 kg ballast anchor at the lower end. The buoyancy unit also included an Iridium GPS transmitter in order to track the drifter during the deployment. Between the buoyancy unit and the ballast anchor, 4-7 Saarso single sediment traps were attached. The water depth at which sediment traps were deployed varied with bottom water depth. At water depths > 1000 m, the sediment traps were generally installed at water depths of 50 m, 100 m, 200 m, 300 m, 400 m and 500 m (see Table 3 for further details).

Table 1 List of drifter-related cruises.

Cruises	Start	End	Season	Ports of embarkation and arrival
M153	2019-02-15	2019-03-31	Summer 2019	Walvis Bay, Namibia – Mindelo, Cape Verde
SO283	2021-03-19	2021-05-25	Autumn 2021	Emden – Emden, Germany
SO285	2021-08-20	2021-11-02	Spring 2021	Emden – Emden, Germany

In order to prevent biological activity and degradation in the sample cups and to reduce exchange with the surrounding water, the water in the cups was poisoned with $HgCl_2$ (3.3 g/l) and enriched with salt (NaCl 70 g/l) before the deployment. In this way, the samples remain in the same condition as they were during the periods of deployment until the actual analysis: cooled, darkened and poisoned with $HgCl_2$. It has been accepted since the early 1980s that the addition of a toxin to sediment trap samples prevents bacterial or microbial degradation of the material (see e.g. Honjo et al., 1982). Metfies et al. (2017) have even found that PCR-based molecular genetic analysis is possible in sediment trap samples from long-term moorings when the samples have been poisoned with $HgCl_2$. After recovery, all samples were stored at 4°C on the ship and either examined directly on board or transported immediately to the home laboratory at the University of Hamburg, Germany, without interruption of cooling.

In general, all sediment trap samples were first macroscopically described and then divided into two fractions (> 1 mm and < 1 mm) using a 1x1 mm mesh size sieve. The > 1 mm fraction is classified as active swimmers (Lee

et al., 1988, 1991). The < 1 mm fraction represents the passive flux. Haake et al. (1993) and Rixen et al. (1996) described in detail the processing and analysis of sediment trap samples. Both the preparation of the sampling cup before deployment and the processing of the samples after recovery were carried out according to generally accepted procedures (e.g., Honjo et al., 1982 Honjo et al. 2008, Metfies et al., 2017). The > 1mm fraction of the long-term moorings will be discussed in a future work.

Table 2 Overview of moored sediment trap deployments.

Station	Mooring No	Latitude [°S]	Longitude [°E]	Water Depth [m]	Trap Depth [m]	Start	End	Sampling Interval [days]
nBUS	1	-23.0000	14.0800	140	70	2009-12-15	2010-08-26	21
nBUS	2	-22.6000	14.2000	127	60	2010-11-27	2010-12-09	12
nBUS	3	-23.0225	14.0277	130	75	2013-07-04	2013-07-31	30
nBUS	4	-23.0248	14.0370	130	75	2014-05-14	2014-06-03	21
nBUS	6	-23.0165	14.0368	130	75	2016-04-25	2016-05-24	29
nBUS	7	-23.0173	14.0368	130	75	2017-04-26	2017-05-25	29
nBUS	8	-23.0231	14.2185	110	65	2019-10-21	2019-11-30	40
nBUS	9	-23.0229	14.0370	130	75	2021-07-01	2021-07-13	12
nBUS	10	-23.0232	14.0370	130	75	2021-11-29	2021-12-08	9
nBUS	11	-23.0233	14.0371	130	75	2022-07-22	2022-08-21	30
sBUS	1	-30.6367	17.0158	170	95	2019-10-21	2019-11-20	30
sBUS	2	-30.6374	17.0172	170	95	2021-07-02	2021-07-14	12
sBUS	3	-30.6378	17.0175	170	95	2022-03-24	2022-04-23	30

Table 3 Overview of drifter deployments.

Region	Cruise ID	Drifter	Water depth (m)	Deployment [UTC]	Recovery [UTC]	Dep. Lat [°S]	Dep. Lon [°E]	Rec. Lat [°S]	Rec. Lon [°E]	Drift Distance [km]	Number of Traps	Trap Depth [m]
nBUS	M153	1	2050	2019-03-03 22:36	2019-03-05 16:33	22.9996	12.2489	22.9358	12.1475	15.4	5	50, 100, 200, 300, 500
nBUS	M153	2	1000	2019-03-06 22:18	2019-03-10 10:30	20.9999	11.9992	20.8942	11.9064	29.7	5	30, 50, 100, 150, 200
sBUS	M153	3	1300	2019-02-22 18:51	2019-02-25 12:13	31.0440	15.2280	30.9683	15.095	20.5	5	50, 100, 200, 300, 500
sBUS	M153	4	160	2019-02-18 11:07	2019-02-20 08:27	30.6417	17.0226	30.5275	16.8453	24.4	4	20, 30, 50, 75
sBUS	SO283	5	997	2021-04-15 19:58	2021-04-17 12:33	31.4987	15.4980	31.4802	15.4353	8.5	6	50, 100, 200, 300, 400, 500
sBUS	SO283	6	192	2021-04-16 09:15	2021-04-18 05:52	30.9998	16.9998	31.0366	16.9735	11.4	5	20, 30, 50, 75, 100
nBUS	SO283	7	1155	2021-04-21 09:16	2021-04-23 14:26	23.0001	12.7496	22.9750	12.6905	9.4	5	50, 100, 300, 400, 500
nBUS	SO283	8	248	2021-04-21 05:49	2021-04-23 10:19	23.0001	13.5833	22.9887	13.4818	15.6	5	20, 30, 50, 75, 100
nBUS	SO283	9	732	2021-04-24 14:41	2021-04-25 15:07	17.9998	11.3001	17.9641	11.3210	5.6	7	10, 50, 100, 200, 300, 400, 500
nBUS	SO283	10	360	2021-04-27 10:57	2021-04-29 11:19	25.0004	13.9151	24.868	13.6998	22.1	5	20, 30, 50, 75, 100
nBUS	SO283	11	1045	2021-04-27 04:59	2021-04-29 06:00	25.0002	13.3333	24.8684	13.2678	18.1	4	50, 100, 300, 400
sBUS	SO285	12	1097	2021-09-19 02:50	2021-09-19 15:48	31.9298	15.7738	31.9298	15.7738	1.91	5	20, 50, 100, 150, 200
sBUS	SO285	13	155	2021-09-21 01:22	2021-09-21 14:44	30.9962	17.3493	30.9180	17.3133	9.95	5	20, 30, 50, 75, 100
sBUS	SO285	14	1047	2021-09-24 07:57	2021-09-25 14:15	30.3525	14.5834	30.3296	14.4208	17.8	6	50, 100, 200, 300, 400.0, 500
nBUS	SO285	15	1888	2021-10-01 19:35	2021-10-02 15:35	22.9981	12.3988	22.8982	12.4168	18.01	6	50, 100, 200, 300, 400, 500
nBUS	SO285	16	517	2021-10-05 07:19	2021-10-07 12:01	21.0223	12.4218	20.7052	12.4466	35.97	5	20, 50, 100, 150, 200

205

For the drifter samples, the fraction > 1 mm was analysed for active simmers by the use of Keyence VHX-6000 digital microscope. It should be noted that there are currently no definitive, generally standardised methods for quantifying the proportion of migrating zooplankton that has actively entered the sediment trap. However, methods such as that of Weldrick et al. (2021), where the active organisms were hand-picked to quantify their abundance in drifting sediment trap samples, provide approaches dealing with active swimmers in drifting sediment trap samples; this procedure is similar and comparable to the approach used in this study. After removing swimmers from the > 1mm fraction, they were classified according to Tutasi and Escribano (2020), Ekau et al. (2018) and Castellani and Edwards (2017). Furthermore, zooplankton > 1 mm without any signs of decay or disintegration were classified as swimmers and included to the active flux. Zooplankton that showed clear signs of degradation or disintegration were considered part of the passive flux, as we assumed these organisms were dead when they entered the trap.

The active flux (i.e., swimmers) were divided into eight groups: amphipoda, copepoda, decapoda, euphausiacea, ostracoda, pteropoda, fish larvae and gelatinous zooplankton. Swimmers which could not be further classified were therefore classified as 'zooplankton unknown'.

Subsequently, all trap samples used for further analyses were taken on polycarbonate filters (Millipore, 0.45 µm mesh size). The samples were rinsed with a sodium tetraborate buffer solution (2 mg $Na_2[B_4O_5(OH)_4]$ $8H_2O$ per 1 litre H_2O) to remove salt and prevent dissolution of carbonates. After filtration, the filters were dried at 40°C for 48 hours and weighed to determine the dry weight in each zooplankton group and of the < 1 mm fraction. The dried material was carefully removed from the filters with a spatula in order to prevent contamination of the sample by filter material. All filters were thoroughly visually inspected to ensure that no sample material larger than 0.45 µm (mesh size of the polycarbonate filter) remained on the filter surface. Virtually blank filters were left behind, thus preventing size fractionation. The material was then homogenised using an agate mortar and pestle and subsequently analysed for total carbon (TC) and total nitrogen (TN). POC was measured in a second run of samples in which inorganic carbon was removed by acidification (1N HCl). All analyses were carried out using the flash combustion method (Euro Vector EA-3000). Due to the lack of sufficient sample material, e.g., when analysing swimmers, it was often only possible to determine the TC. As swimmers contain almost no carbonate apart from pteropods, the measured TC was interpreted as POC. This leads to a potential overestimation of the active POC flux, but given the relatively low abundance of this zooplankton clade, as shown in the results section, we expect this error to be negligible. The active and the passive POC flux together give the total POC flux. The POC flux multiplied by 1.8 (Anderson, 1995, Francois et al., 2002) results in the organic matter (OM) flux.

Satellite-derived monthly mean sea surface temperature (SST, Reynolds et al., 2002) and net primary production rates (Behrenfeld and Falkowski, 1997) were downloaded from the OI-SST website (http://iridl.ldeo.columbia.edu/SOURCES/.NOAA/.NCEP/.EMC/.CMB/.GLOBAL/.Reyn_SmithOIv2/.monthly/. sst/) and the Ocean Primary Production website (http://www.science.oregonstate.edu/ocean.productivity/) in November 2023. The SST data with a spatial resolution of 0.33x0.33 degrees covered the period from 1981 to 2023, while the primary production rates with a resolution of 1x1 degrees covered the periods from 2002 to 2023. When calculating the mean values for the BUS and the two subsystems, it was assumed that the BUS covers the area between the coast and about 250 km offshore, within the latitudes we have previously specified (nBUS 17-27°S and sBUS 27°-35°S, see Fig.1).

Results

During the research cruises, the primary production rates at the coast reached values of > 9000 mg m^{-2} day^{-1}, which decreased with increasing distance from the coast and fell to values of < 10 mg m^{-2} day^{-1} far offshore (Fig. 4). The primary production rates at the drifter positions varied between 544.6 mg m^{-2} day^{-1} and 5115.4 mg m^{-2} day^{-1} and revealed a mean of 1618.6 ± 1110.6 mg m^{-2} day^{-1}. They thus fell below the average primary production rates, which 250 were 2505.3 mg m^{-2} day^{-1} in the nBUS and 2089.6 mg m^{-2} day^{-1} in the sBUS (Fig. 3b). Overall, the primary production derived from the satellite data largely fell within the range of primary production rates determined during research cruises in winter 1999 and summer 2002 in the sBUS and nBUS ($140 - 8830$ mg m^{-2} day^{-1} Barlow et al., 2009).
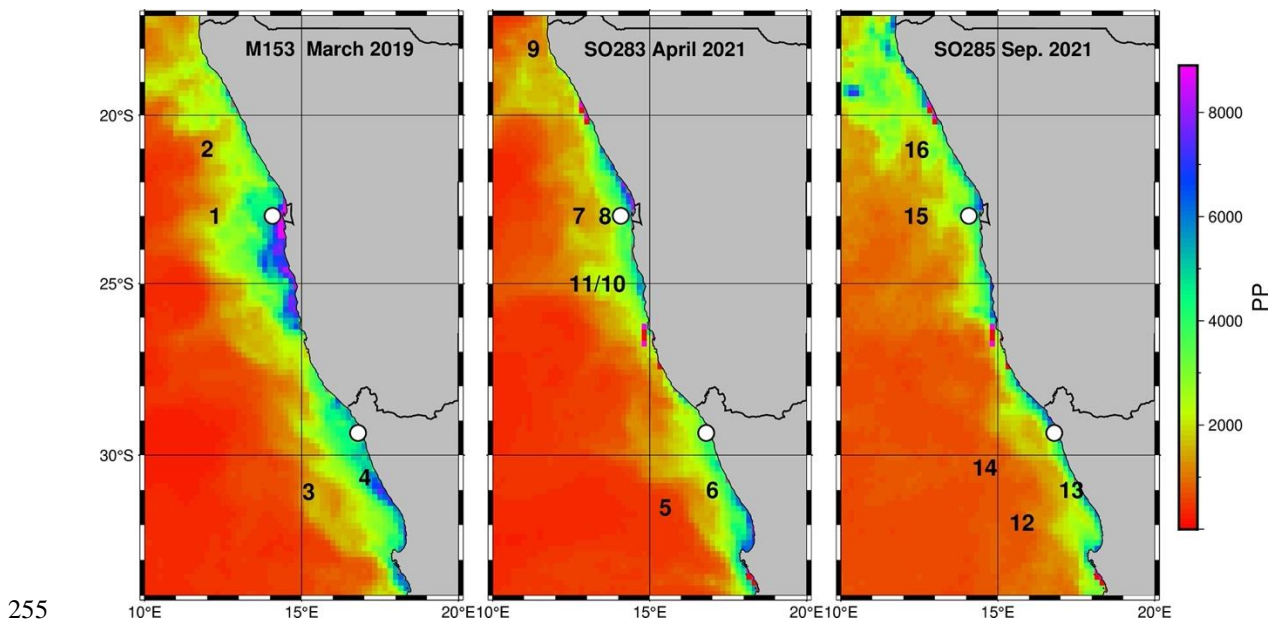
Figure 4 Primary production rates (SeaWiFS) in mg C m^{-2} day^{-1} during the research cruises M153, SO283 and SO285 as well as the locations of the drifters deployments (black numbers) and long-term sediment trap mooring sites (white circles).

The results from the 83 drifter traps showed that copepod biomass accounts for the largest proportion of the active POC flux in both subsystems averaged over all water depths (55.7 % and 46.2 % in the nBUS and sBUS), followed 260 by the biomass of amphipods and euphausiids (Fig. 5). The combined proportion of the three groups (copepods, amphipods and euphausiids) amount to about 77.3 % and 87.4 % of the active POC in the nBUS and sBUS.
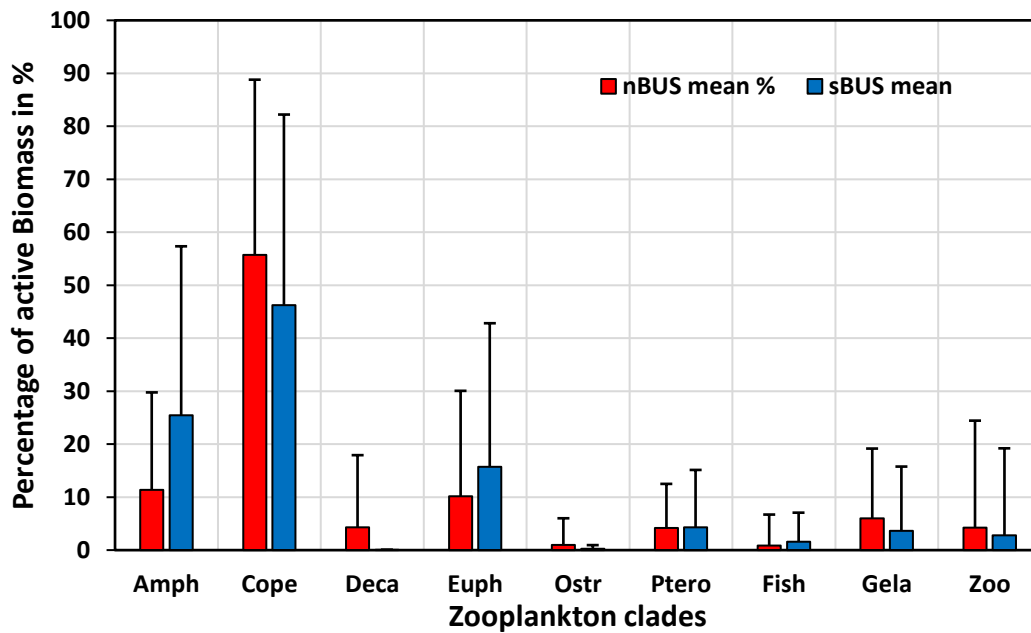
Figure 5 Proportion of zooplankton groups in the active POC averaged over all traps with a mean standard deviation of 15±8%. Amph- amphipods, Cope- copepods, Deca – decapoda, Euph- euphausiids, Ostr- ostracodes, Ptero- pteropods, Fish- fish larvae, Gela – gelatinous organisms, Zoo- zooplankton not further identified.

Averaged over all sampled water depths and drifter deployments in both subsystems the proportion of the active POC flux to the total POC flux was on average 10.9% higher in the sBUS (mean: 72.9 %) than in the nBUS (mean: 62.0 %) and varied with depth by ± 14.2 % (nBUS) and ± 9.0 % (sBUS). However, the active POC flux of 944.5 ± 743.6 mg m^{-2} day^{-1} in the sBUS was 2.9 times higher than in the nBUS with 322 ± 231.7 mg m^{-2} day^{-1}. This difference was particularly visible in the upper water column (water depths < 100 m), and decreased in greater water depths where the active POC flux in nBUS could even exceed that in the sBUS (Fig. 7a).
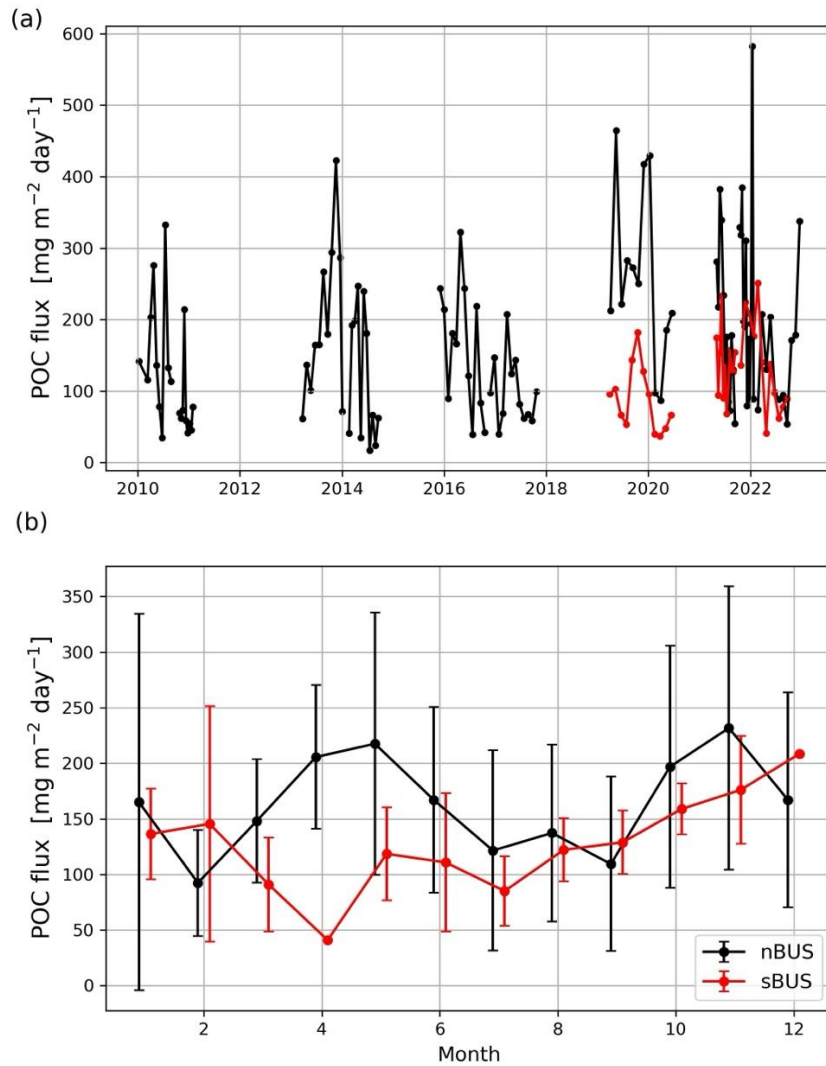
Figure 6 POC flux rates measured off Walvis Bay in the nBUS and Hondeklip Bay in the sBUS moorings (a) and the mean annual cycle (b) derived from the mooring data shown in (a).

275   Compared to the active POC flux, the passive POC flux in the sBUS is only slightly higher (293.9 $\pm$ 249.0 mg m^{-2} day^{-1}) than in the nBUS (203.1 $\pm$ 157.0 mg m^{-2} day^{-1}). The passive POC flux tends to decrease with depth (Fig. 7b) and shows an average POC flux of 135.9 $\pm$ 82.3 mg m^{-2} day^{-1} (nBUS) and 365.1 $\pm$187.3 mg m^{-2} day^{-1} (sBUS) at a water depth of 100 m. In contrast, the POC flux in the moored traps averaged over the entire observation period in the nBUS at a water depth of 64 m (moored trap depth) and in the sBUS at a water depth of

280   about 100 m (moored trap depth) was 169.8 $\pm$ 128.6 mg m^{-2} day^{-1} and 120.1 $\pm$ 55.8 mg m^{-2} day^{-1}, respectively. The data from the moored sediment traps showed no clear seasonal variability, but in the nBUS there was significant interannual variability (Fig. 5). However, our time series in the sBUS is still too short to make statements about interannual variability.
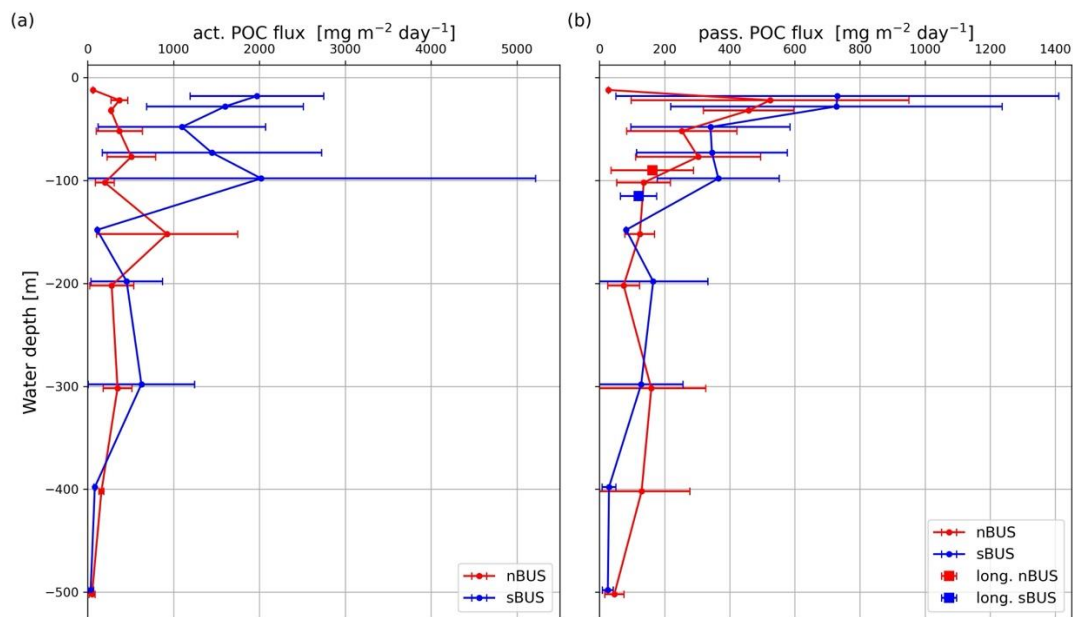
Figure 7 Active (a) and passive POC flux (b) averaged over all traps deployed at the same water depth versus water depth, including mean passive POC flux rates (squares) of the long-term moorings in the nBUS and sBUS.

Discussion

The drifters were deployed on the shelf and along the continental slope at the beginning and end of the summer season. However, as mentioned before, the drifters were deployed in areas where the primary production was on average below the mean summer primary production and it ranged between 544.6 and 5114.4 mg m^{-2} day^{-1}. The active and passive POC flux in the upper water column (water-depth < 100 m) varied between 45.3 and 9121.2 mg m^{-2} day^{-1} and 8.8 – 1878 mg m^{-2} day^{-1} respectively. This means that the variability of the active POC flux exceeded that of primary production, and the variability of the passive POC flux, which is comparatively low, still extends over three orders of magnitude (Fig. 7b). These large variations are the product of the interaction between the oceanographic processes that influence the transport of nutrients into the euphotic zone, their horizontal distribution in the surface water and biological processes that convert the nutrients into biomass and export them as POC. Our data density is not sufficient to disentangle this complex interaction completely, but on average the sediment trap results agree well with the results of other studies. For instance, vertical hauls down to a water depth of 600 m with a Hydro-Bios Multi Plankton Sampler in the Humboldt Upwelling System off northern Chile yielded a mean biomass of migrating zooplankton of 958 mg C m^{-2} day^{-1} (Tutasi and Escribano, 2020), which is quite similar to the mean active POC flux derived from our drifter trap samples (944.5 ± 743.6 mg m^{-2} day^{-1} in the sBUS and 322 ±- 231.7 mg m^{-2} day^{-1} in nBUS). In the California Upwelling System, the active and passive POC flux at a water depth of 100 m was estimated at 34.8 and 108.0 mg m^{-2} day^{-1}, respectively (Stukel et al., 2023). This active POC flux is below the mean flux we have measured in nBUS at a water-depth of 100 m (200 ± 108 mg m^{-2} day^{-1}) but it falls in the range of the active flux we have determined in the sBUS (2022.1 ± 3195 mg m^{-2} day^{-1}) at a water-depth of 100 m (Fig. 7a). The passive flux off California, on the other hand, is in the range of what we have measured with the drifter in the nBUS (135.8 ± 82 mg m^{-2} day^{-1}, Fig. 7b) but falls below what was measured in the sBUS (365.1 ±187.2 mg m^{-2} day^{-1}, Fig. 7b). Overall, our results are in good agreement with those from other eastern boundary upwelling systems.

Our sediment trap results show furthermore that copepods dominate the active POC flux in both subsystems (Fig. 5), which is consistent with biological studies revealing that copepods dominate the abundance of mesozooplankton in the nBUS and sBUS (Verheye et al., 2016; Bode et al., 2014). This implies that copepods in the BUS not only play a key role as a food source for the conservation of marine fish stocks, but are also of great importance for the active POC flux. This in turn raises the question of how the active flux affects the passive POC flux and the associated POC transport onto the sediments.

Zooplankton influence the passive POC flux to the sediment in many ways, which can increase or decrease the active POC flux (Steinberg and Landry, 2017, Boyd et al., 2019, Moigne 2019 and Miles, 2018). Grazing and disaggregation are e.g., processes that decrease the passive POC flux while excretion of faecal pellets and the death of zooplankton increase the passive POC flux (Cavan et al., 2020, Turner, 2014, Ducklow et al., 2001). In the sBUS, the active POC flux was almost 3 times higher than in the nBUS, which was most pronounced in the upper water column (water depth < 150 m, Fig 7 a), while the passive POC flux did not differ greatly between the two subsystems (Fig. 7b). This implies that the role of zooplankton on the passive POC flux varied in the two subsystems.

On average, the passive POC flux decreases with depth as commonly observed in other studies and has been described by a POC flux attenuation equation (Cael and Bisson, 2018; Martin et al., 1987; Giering et al., 2014). To ensure comparability with other regions, we have selected the commonly used equation (Eq. 1, Martin et al. 1987) for describing the POC flux attenuation at increasing water-depth and adapt it to the situation found in the BUS (Fig. 8).

The selected MLD as well as the determined FMLD and 'b' values were then used to calculate the POC fluxes using the Martin curve and the water depth. The calculated and measured POC fluxes correlated with each other (r = 0.925, n = 31) and showed the best agreement at an assumed MLD of approximately 10 m. The values for FMLD and 'b' obtained from the curve fitting were 1117 mg C m-2 day-1 and -0.74 (Fig. 8). Temperature profiles obtained during our expeditions at our long-term sediment trap sites showed that MLDs in the nBUS and sBUS varied between approximately 30 m and 15 m during the austral spring (Fig. 9a). In late summer, the mean depth varied between about 1 m and 14 m (Fig. 9b), showing that an MLD of 10 m, as assumed for the curve fitting, is within the range observed during our expeditions.

If the 'b' is reduced to -0.86, the resulting POC flux attenuation curve represents the long-term sediment trap data off Walvis Bay in nBUS and Hondeklip Bay in sBUS significantly better. However, 'b' values of -0.74 and -0.86 are in the range of the 'b' values found in the Pacific Ocean and the Atlantic Ocean (b = -0.5 to -1.38; Giering et al., 2014) and similar to those determined in the California upwelling system (b = -0.72, Stukel et al., 2023). The calculated POC flux rates also agree well with those measured in previous sediment trap studies in the BUS at water depth > 500 m (Fig. 8a, Vorrath et al., 2018).
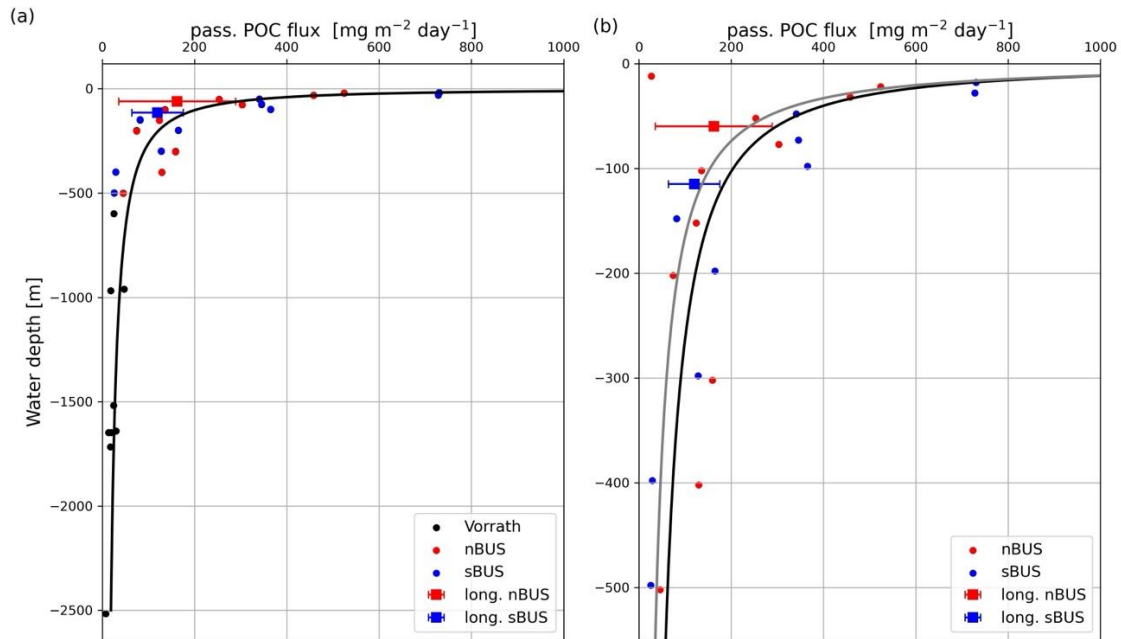
345 **Figure 8** Mean POC flux rates (red and blue dots) versus water depths of 0 m - 2500 m (a) and 0 m - 500 m (b). The curves are Martin curves with a 'b' of -0.74 (black) and -0.86 (grey). The result of an nBUS trap at 10 m water depth (see b, red circle at 10 m depth) was not considered in the curve fitting. Sediment trap data (black dots) taken from Vorrath et al. (2018); squares depict the mean POC flux of the long-term moorings from this study.

The determined F_{MLD} implies a mean export production of 1117 mg C m^{-2} day^{-1}. Compared to the primary

350 production rates of 2089 mg C m^{-2} day^{-1} (sBUS) and 2505 mg C m^{-2} day^{-1} (nBUS) this indicates an f-ratio (=export production/primary production) of approximately 0.4 to 0.5 which is characteristic of highly productive systems (Eppley and Peterson, 1979). This means that the passive POC flux determined with drifters and long-term sediment traps (on the shelf and in the open ocean) appears to follow the general attenuation equations on average, despite the large variations of the individual measurements.

355
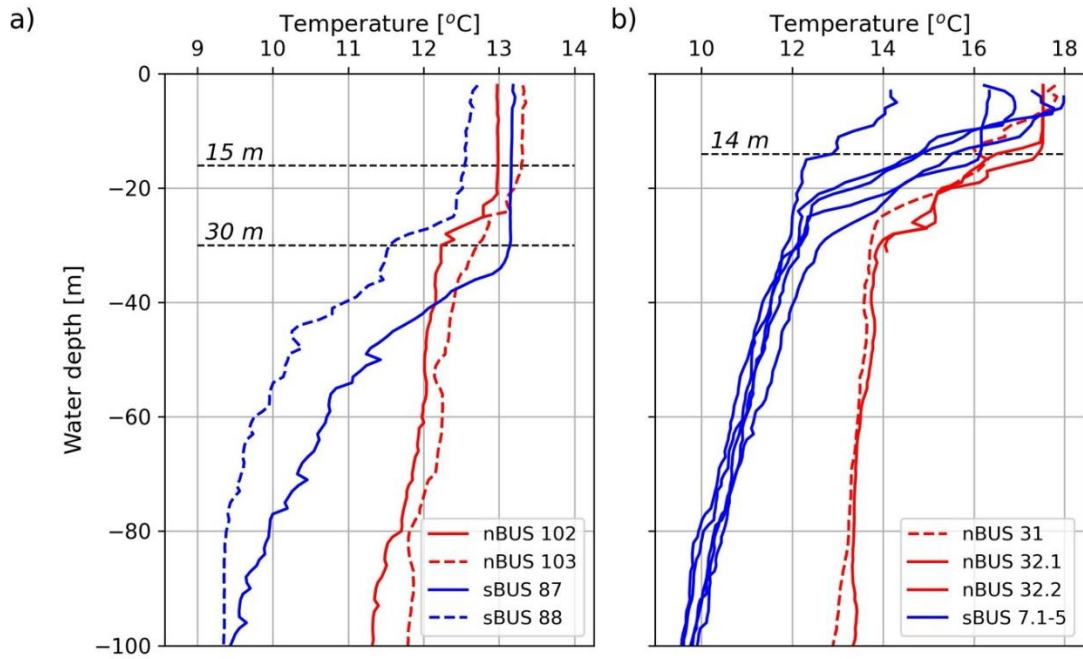
Figure 9 Temperature profiles at the CTD stations (depth resolution of 1 m) closest to the long-term mooring site during the cruises SO285 austral spring (a) and M153 austral summer (b). The positions of the mooring stations are shown in Fig. 1 and Tab.1. Decimal places indicate that there have been several casts at the stations. Station 7 was a long station at which five CTD casts have been carried out over the course of a day. It should be noted that the MLD at station 7 showed a diurnal variation, with a maximum depth of approx. 14 meters. A maximum MLD of approx. 14 m was also shown in the nBUS (station 32). During the SO285 cruise in austral spring, the MLDs varied between approx. 30 m and 15 m. The dashed lines were inserted to illustrate the maximum MLDs. CTD data available at https://www.pangaea.de.

Assuming a mean water depth of 150 m, which is based on the mean depth of the continental shelf, the derived Martin equations (b of -0.74 and -0.86, respectively) suggest a POC supply to sediments of 108.8 - 152.0 mg C m^{-2} day^{-1}. Compared to the primary production rate this implies that 4 – 7 % of primary produced POC reaches the sediment. This is consistent with our former result of 5 % based on the long-term sediment trap study off Walvis Bay and contradicts the results of a numerical model, which states that 49 % of the primary produced POC reaches the sediment surface (Emeis et al., 2018). However, the similar POC fluxes in nBUS and sBUS are remarkable, especially considering the differences in the active POC flux and the OMZ intensity (Fig.10).
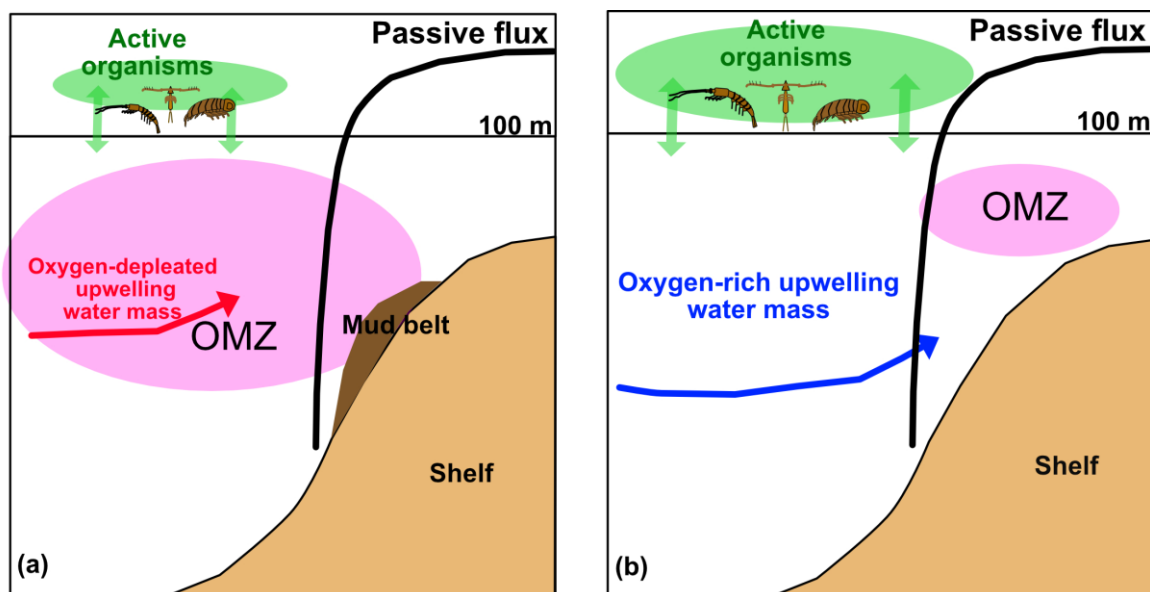
Figure 10 System schematics in the nBUS (a) and the sBUS (b). Green arrows and their size characterize the active transport pathways. The black curve shows the Martin curve based passive POC flux which is similar in both systems. Red and blue
375 arrows show the contribution and entering of upwelling source water masses. The dark brown area indicates the POC-rich mud belt in the nBUS which is absent in the sBUS.

Low oxygen concentrations and the associated transition from oxic to anoxic degradation processes are considered to be a factor that reduces POC degradation in the water column and surface sediments (Paropkari et al., 1993; Laufkötter et al., 2017) and also increase the quality of the preserved organic matter in the nBUS (Nagel et al.,
380 2016). If lower oxygen concentrations in the nBUS have a positive effect on the POC flux, but this flux, including export production, is almost similar to that in the sBUS, there are probably also processes that, similar to the low oxygen concentration in the nBUS, favour the passive POC flux in the sBUS. Since the active POC flux in the upper water column is significantly higher in the sBUS than in the nBUS (Fig. 7a), zooplankton is assumed to play this role. As primary production and export production rates are similar in both subsystems, high zooplankton
385 abundance is expected to favour passive POC fluxes by enhancing the production of fast-sinking faecal pellets in the sBUS. As mentioned above, the attenuation coefficient 'b' is an expression of the strength of remineralisation. According to our results, 'b' is similar in both subsystems, which leads to the assumption that the effect of a lower oxygen concentration on 'b' in the nBUS is comparable to the effect of zooplankton on 'b' in the sBUS. One way in which zooplankton may contribute is by increasing the formation of rapidly sinking faecal pellets and reducing
390 the residence time of sinking particles in the water column. This would mean that the positive effect on passive POC flux caused by higher zooplankton abundance would overcompensate for negative effects such as increased disaggregation of sinking particles due to grazing at our study sites.

In the water column, however, the effects of POC degradation processes on the distribution of nutrients and dissolved inorganic carbon are masked by the inflow of different upwelling source waters in the two subsystems
395 as illustrated in Figure 10. As mentioned above, and shown by Siddiqui et al. (2023), source waters in the nBUS are not only oxygen depleted and nutrient enriched but also enriched in dissolved inorganic carbon (DIC). The much more pronounced OMZ in the nBUS, in addition to the almost equal POC fluxes in both subsystems and the high sedimentary POC concentrations in the nBUS (Fig. 1), also indicates that the mud belt in the nBUS is largely a consequence of the stronger OMZ in the nBUS compared to the sBUS. This highlights the ambivalent nature of

19

400 expanding OMZs, which mitigates atmospheric and oceanic CO_2 accumulation by increasing POC storage in sediments and poses a threat to established ecosystems and fisheries.

Summary

Our results indicate that the large variability of the measured POC fluxes reflects the expected spatial and temporal variability of the BUS. On average, however, and in agreement with other studies, our results show that copepods

405 dominate zooplankton abundance and the active POC flux in both subsystems. The active POC flux in the sBUS was almost 3 times higher than the nBUS. This difference was particularly evident in the upper 100 to 150 m of the water column. In contrast to the active POC flux, the passive POC flux was almost the same in both subsystems and followed in accordance with the long-term sediment trap data the general attenuation equations on average, despite significant deviation of the individual measurements. A similar POC export production and attenuation

410 with increasing water depth, in addition to a more pronounced OMZ in the nBUS and a much higher zooplankton abundance in the sBUS implies that both, the low oxygen concentrations and the higher zooplankton abundance, favour the passive POC flux at our study sites. The former is well accepted while the latter means that zooplankton reduce POC remineralization by increasing the particle sinking speed. This, in turn, suggests that increased formation of fast-sinking faecal pellets overcompensates for enhanced grazing on sinking particles that favours

415 particle disaggregation and reduces the sinking speed. Similar productivity and POC supply but large differences in POC concentration and storage in the surface sediments of the nBUS and sBUS suggest that the intensity of the OMZ is key to understanding the development of the POC-rich mud belt in the nBUS which is absent in the sBUS.

References

Anderson, L. A.: On the hydrogen and oxygen content of marine phytoplankton, Deep-Sea Research Part I-
445   Oceanographic Research Papers, 42, 1675-1680, 10.1016/0967-0637(95)00072-e, 1995.

Archibald, K. M., Siegel, D. A., and Doney, S. C.: Modeling the Impact of Zooplankton Diel Vertical Migration on the Carbon Export Flux of the Biological Pump, Global Biogeochemical Cycles, 33, 181-199, 10.1029/2018GB005983, 2019.

Atwood, T. B., Witt, A., Mayorga, J., Hammill, E., and Sala, E.: Global Patterns in Marine Sediment Carbon
450   Stocks, Frontiers in Marine Science, 7, 165, 2020.

Bailey, G. W.: Organic carbon flux and development of oxygen deficiency on the modern Benguela continental shelf south of 22°S: Spatial and temporal variability, in: Modern and Ancient Continental Shelf Anoxia, edited by: Tyson, R. V., and Pearson, T. H., Geological Society, London, UK, 171– 183, 1991.

Bakun, A.: Climate change and ocean deoxygenation within intensified surface-driven upwelling circulations,
455   Philosophical Transactions of the Royal Society A: Mathematical, Physical and Engineering Sciences, 375, 20160327, 10.1098/rsta.2016.0327, 2017.

Barlow, R., Lamont, T., Mitchell-Innes, B., Lucas, M., and Thomalla, S.: Primary production in the Benguela ecosystem, 1999 - 2002, African Journal of Marine Science, 31, 97-101, 10.2989/ajms.2009.31.1.9.780, 2009.

460   Behrenfeld, M. J. and Falkowski, P. G.: Photosynthetic rates derived from satellite-based chlorophyll concentration, Limnology and Oceanography, 42, 1-20, 1997.

Bianchi, D., Carozza David, A., Galbraith Eric, D., Guiet, J., and DeVries, T.: Estimating global biomass and biogeochemical cycling of marine fish with and without fishing, Science Advances, 7, eabd7554, 10.1126/sciadv.abd7554, 2021.

465   Bianchi, D., Galbraith, E. D., Carozza, D. A., Mislan, K. A. S., and Stock, C. A.: Intensification of open-ocean oxygen depletion by vertically migrating animals, Nature Geosci, 6, 545-548, 2013.

Bode, M., Kreiner, A., van der Plas, A. K., Louw, D. C., Horaeb, R., Auel, H., and Hagen, W.: Spatio-Temporal Variability of Copepod Abundance along the 20°S Monitoring Transect in the Northern Benguela Upwelling System from 2005 to 2011, PLOS ONE, 9, e97738, 10.1371/journal.pone.0097738, 2014.

470   Bordbar, M. H., Mohrholz, V., and Schmidt, M.: The Relation of Wind-Driven Coastal and Offshore Upwelling in the Benguela Upwelling System, Journal of Physical Oceanography, 51, 3117-3133, 10.1175/JPO-D-20-0297.1, 2021.

Boyd, P. W., Claustre, H., Levy, M., Siegel, D. A., and Weber, T.: Multi-faceted particle pumps drive carbon sequestration in the ocean, Nature, 568, 327-335, 10.1038/s41586-019-1098-2, 2019.

475   Cael, B. B. and Bisson, K.: Particle Flux Parameterizations: Quantitative and Mechanistic Similarities and Differences, Frontiers in Marine Science, 5, 2018.

Cavan, E. L., Henson, S. A., Belcher, A., and Sanders, R.: Role of zooplankton in determining the efficiency of the biological carbon pump, Biogeosciences, 14, 177-186, 10.5194/bg-14-177-2017, 2017.

Carr, M.-E.: Estimation of potential productivity in Eastern Boundary Currents using remote sensing, Deep Sea
480   Research Part II: Topical Studies in Oceanography, 49, 59-80, 2001.

Castellani, C. and Edwards, M.: Marine Plankton: A Practical Guide to Ecology, Methodology, and Taxonomy, Limnology and Oceanography Bulletin, 26, 704, https://doi.org/10.1002/lob.10199, 2017.

Chavez, F. P. and Messié, M.: A comparison of Eastern Boundary Upwelling Ecosystems, Progress in Oceanography, 83, 80-96, 2009.

485   Chavez, F. P. and Toggweiler, J. R.: Physical estimates of global new production: The upwelling contribution, in: Upwelling in the ocean, modern processes and ancient records, edited by: Summerhayes, C. P., Emeis, K.-C., Angel, M. V., Smith, R. L., and Zeitschel, B., Wiley & Sons, Chichester, 313-320, 1995.

Cockcroft, A. C.: Jasus lalandii 'walkouts' or mass strandings in South Africa during the 1990s: an overview, Marine and Freshwater Research, 52, 1085-1093, 2001.

490   Cockcroft, A. C., van Zyl, D., and Hutchings, L.: Large-scale changes in the spatial distribution of South African West Coast rock lobsters: an overview, African Journal of Marine Science, 30, 149-159, 10.2989/AJMS.2008.30.1.15.465, 2008.

del Giorgio, P. A. and Duarte, C. M.: Respiration in the open ocean, Nature, 420, 379-384, 2002.

DeVries, T. and Deutsch, C.: Large-scale variations in the stoichiometry of marine organic matter respiration,
495   Nature Geosci, 7, 890-894, 2014.

Ducklow, H. W., Steinberg, D. K., and Buesseler, K. O.: Upper ocean carbon export and the biological pump, Oceanography, 14, 50-58, 10.5670/oceanog.2001.06, 2001.

Duce, R. A., LaRoche, J., Altieri, K., Arrigo, K. R., Baker, A. R., Capone, D. G., Cornell, S., Dentener, F., Galloway, J., Ganeshram, R. S., Geider, R. J., Jickells, T., Kuypers, M. M., Langlois, R., Liss, P. S., Liu, S.
500   M., Middelburg, J. J., Moore, C. M., Nickovic, S., Oschlies, A., Pedersen, T., Prospero, J., Schlitzer, R., Seitzinger, S., Sorensen, L. L., Uematsu, M., Ulloa, O., Voss, M., Ward, B., and Zamora, L.: Impacts of Atmospheric Anthropogenic Nitrogen on the Open Ocean, Science, 320, 893-897, 10.1126/science.1150369, 2008.

Ekau, W., Auel, H., Hagen, W., Koppelmann, R., Wasmund, N., Bohata, K., Buchholz, F., Geist, S., Martin, B.,
505   Schukat, A., Verheye, H. M., and Werner, T.: Pelagic key species and mechanisms driving energy flows in the northern Benguela upwelling ecosystem and their feedback into biogeochemical cycles, Journal of Marine Systems, 188, 49-62, https://doi.org/10.1016/j.jmarsys.2018.03.001, 2018.

Emeis, K., Eggert, A., Flohr, A., Lahajnar, N., Nausch, G., Neumann, A., Rixen, T., Schmidt, M., Van der Plas, A., and Wasmund, N.: Biogeochemical processes and turnover rates in the Northern Benguela Upwelling
510   System, Journal of Marine Systems, 188, 63-80, https://doi.org/10.1016/j.jmarsys.2017.10.001, 2018.

Eppley, R. W. and Peterson, B. J.: Particulate organic-matter flux and planktonic new production in the deep ocean, Nature, 282, 677-680, 10.1038/282677a0, 1979.

European Marine Board: Blue Carbon: Challenges and opportunities to mitigate the climate and biodiversity crises., EMB Policy Brief N°. 11, 2023, doi: https://doi.org/10.5281/zenodo.8314215. ISSN: 0778-3590
515   ISBN: 978946420, 2023.

Flohr, A., van der Plas, A. K., Emeis, K.-C., Mohrholz, V., and Rixen, T.: Spatio-temporal patterns of C : N : P ratios in the northern Benguela upwelling regime, Biogeosciences, 11, 885 - 897, doi:10.5194/bg-11-885-2014, 2014., 2014.

Flynn, R. F., Granger, J., Veitch, J. A., Siedlecki, S., Burger, J. M., Pillay, K., and Fawcett, S. E.: On-Shelf
520   Nutrient Trapping Enhances the Fertility of the Southern Benguela Upwelling System, Journal of Geophysical Research: Oceans, 125, e2019JC015948, https://doi.org/10.1029/2019JC015948, 2020.

Francois, R., Honjo, S., Krishfield, R., and Manganini, S.: Factors controlling the flux of organic carbon to the bathypelagic zone of the ocean, Global Biogeochemical Cycles, 16, 10.1029/2001gb001722, 2002.

Giering, S. L. C., Sanders, R., Lampitt, R. S., Anderson, T. R., Tamburini, C., Boutrif, M., Zubkov, M. V.,
525   Marsay, C. M., Henson, S. A., Saw, K., Cook, K., and Mayor, D. J.: Reconciliation of the carbon budget in the ocean/'s twilight zone, Nature, 507, 480-483, 2014.

Haake, B., Ittekkot, V., Rixen, T., Ramaswamy, V., Nair, R. R., and Curry, W. B.: Seasonality and interannual variability of particle fluxes to the deep Arabian Sea, Deep Sea Research I, 40, 1323-1344, 1993.

Halpern, B. S., Longo, C., Hardy, D., McLeod, K. L., Samhouri, J. F., Katona, S. K., Kleisner, K., Lester, S. E.,
530   O'Leary, J., Ranelletti, M., Rosenberg, A. A., Scarborough, C., Selig, E. R., Best, B. D., Brumbaugh, D. R., Chapin, F. S., Crowder, L. B., Daly, K. L., Doney, S. C., Elfes, C., Fogarty, M. J., Gaines, S. D., Jacobsen, K. I., Karrer, L. B., Leslie, H. M., Neeley, E., Pauly, D., Polasky, S., Ris, B., St Martin, K., Stone, G. S.,

Sumaila, U. R., and Zeller, D.: An index to assess the health and benefits of the global ocean, Nature, 488, 615-620, 10.1038/nature11397, 2012.

535   Honjo, S., Manganini, S. J., Krishfield, R. A., and Francois, R.: Particulate organic carbon fluxes to the ocean interior and factors controlling the biological pump: A synthesis of global sediment trap programs since 1983, Progress in Oceanography, 76, 217-285, http://dx.doi.org/10.1016/j.pocean.2007.11.003, 2008.

Honjo, S., Manganini, S. J., and Cole, J. J.: Sedimentation of biogenic matter in the deep ocean, Deep-Sea Research Part a-Oceanographic Research Papers, 29, 609-625, 10.1016/0198-0149(82)90079-6, 1982.

540   Hutchings, L., van der Lingen, C. D., Shannon, L. J., Crawford, R. J. M., Verheye, H. M. S., Bartholomae, C. H., van der Plas, A. K., Louw, D., Kreiner, A., Ostrowski, M., Fidel, Q., Barlow, R. G., Lamont, T., Coetzee, J., Shillington, F., Veitch, J., Currie, J. C., and Monteiro, P. M. S.: The Benguela Current: An ecosystem of four components, Progress in Oceanography, 83, 15-32, 2009.

Jouffray, J.-B., Blasiak, R., Norström, A. V., Österblom, H., and Nyström, M.: The Blue Acceleration: The
545   Trajectory of Human Expansion into the Ocean, One Earth, 2, 43-54, https://doi.org/10.1016/j.oneear.2019.12.016, 2020.

Kalvelage, T., Jensen, M. M., Contreras, S., Revsbech, N. P., Lam, P., Günter, M., LaRoche, J., Lavik, G., and Kuypers, M. M. M.: Oxygen Sensitivity of Anammox and Coupled N-Cycle Processes in Oxygen Minimum Zones, PLOS ONE, 6, e29299, 10.1371/journal.pone.0029299, 2011.

550   Kämpf, J. and Chapman, P.: The Benguela Current Upwelling System, in: Upwelling Systems of the World, Springer, https://doi.org/10.1007/978-3-319-42524-5_7, 2016.

Lacroix, F., Ilyina, T., Laruelle, G. G., and Regnier, P.: Reconstructing the Preindustrial Coastal Carbon Cycle Through a Global Ocean Circulation Model: Was the Global Continental Shelf Already Both Autotrophic and a CO2 Sink?, Global Biogeochemical Cycles, 35, e2020GB006603,
555   https://doi.org/10.1029/2020GB006603, 2021.

Lahajnar, N., Andrae, A., Beier, S., Heinatz, K., Hirschmann, S., Meiritz, L., Mertens, C., Rose, J., Sabbaghzadeh, B., Schmidt, M., Stake, J., Stiehler, J., and Witting, P. J.: Mooring Rescue, Cruise No. SO283, 19 March 2021 - 25 May 2021, Emden (Germany) - Emden (Germany), Gutachterpanel Forschungsschiffe;, Bonn2510-764X, 1-57, 10.48433/cr_so283, 2021.

560   Lamont, T., Hutchings, L., van den Berg, M. A., Goschen, W. S., and Barlow, R. G.: Hydrographic variability in the St. Helena Bay region of the southern Benguela ecosystem, Journal of Geophysical Research: Oceans, 120, 2920-2944, https://doi.org/10.1002/2014JC010619, 2015.

Laufkötter, C. and Gruber, N.: Will marine productivity wane?, Science, 359, 1103, 2018.

Laufkötter, C., John, J. G., Stock, C. A., and Dunne, J. P.: Temperature and oxygen dependence of the
565   remineralization of organic matter, Global Biogeochemical Cycles, 31, 1038-1050, 10.1002/2017GB005643, 2017.

Le Moigne, F. A. C.: Pathways of Organic Carbon Downward Transport by the Oceanic Biological Carbon Pump, Frontiers in Marine Science, 6, 10.3389/fmars.2019.00634, 2019.

Lee, C., Wakeham, S. G., and Hedges, J. I.: The Measurement of Oceanic Particle Flux - Are "Swimmers" A
570   Problem?, Oceanography, 34-36, 1988.

Lee, C., Hedges, J., and Wakeham, S.: Technical problems with the use of sediment traps - preservation, swimmers, and leaching, in: Symposium Proceeedings - Sediment trap studies in the nordic countries (Vol. 2, pp. 36–48), edited by: Wassmann, P., Heiskanen, A.-S. and Lindahl, O., Kristineberg Marine Biological Station. Nurmijavi, ISBN-952-90-2844-X. 1991.

575   Louw, D. C., van der Plas, A. K., Mohrholz, V., Wasmund, N., Junker, T., and Eggert, A.: Seasonal and interannual phytoplankton dynamics and forcing mechanisms in the Northern Benguela upwelling system, Journal of Marine Systems, 157, 124-134, http://dx.doi.org/10.1016/j.jmarsys.2016.01.009, 2016.

Lovelock, C. E. and Duarte, C. M.: Dimensions of Blue Carbon and emerging perspectives, Biology Letters, 15, 20180781, 10.1098/rsbl.2018.0781, 2019.

580   Lutz, M. J., Caldeira, K., Dunbar, R. B., and Behrenfeld, M. J.: Seasonal rhythms of net primary production and particulate organic carbon flux to depth describe the efficiency of biological pump in the global ocean, Journal of Geophysical Research: Oceans, 112, C10011, 10.1029/2006jc003706, 2007.

Macreadie, P. I., Anton, A., Raven, J. A., Beaumont, N., Connolly, R. M., Friess, D. A., Kelleway, J. J., Kennedy, H., Kuwae, T., Lavery, P. S., Lovelock, C. E., Smale, D. A., Apostolaki, E. T., Atwood, T. B., Baldock, J., Bianchi, T. S., Chmura, G. L., Eyre, B. D., Fourqurean, J. W., Hall-Spencer, J. M., Huxham, M., Hendriks, I. E., Krause-Jensen, D., Laffoley, D., Luisetti, T., Marbà, N., Masque, P., McGlathery, K. J., Megonigal, J. P., Murdiyarso, D., Russell, B. D., Santos, R., Serrano, O., Silliman, B. R., Watanabe, K., and Duarte, C. M.: The future of Blue Carbon science, Nature Communications, 10, 3998, 10.1038/s41467-019-11693-w, 2019.

Martin, J. H., Knauer, G. A., Karl, D. M., and Broenkow, W. W.: VERTEX: carbon cycling in the northeast Pacific, Deep Sea Research, 34, 267-285, 1987.

McCartney, M. S.: Subantarctic Mode Water, in: A Voyage of Discovery: George Deacon 70th Anniversary Volume, edited by: Angel, M. V., Supplement to Deep-Sea Research, Pergamon Press, Oxford, UK, 103 - 119, 1977.

Metfies, K., Bauerfeind, E., Wolf, C., Sprong, P., Frickenhaus, S., Kaleschke, L., Nicolaus, A., and Nöthig, E. M.: Protist Communities in Moored Long-Term Sediment Traps (Fram Strait, Arctic)-Preservation with Mercury Chloride Allows for PCR-Based Molecular Genetic Analyses, Frontiers in Marine Science, 4, 10.3389/fmars.2017.00301, 2017.

Miles, M.: The Biological Carbon Pump: Climate Change Warrior. Berkeley Scientific Journal, 23(1). https://escholarship.org/uc/item/7cg4n7p8, 2018.

Mohrholz, V., Bartholomaeb, C. H., and van der Plas, A. K.: The seasonal variability of the northern Benguela undercurrent and its relation to the oxygen budget on the shelf, Continental Shelf Research, 28, 424 - 441, 2008.

Monteiro, P. M. S., Dewitte, B., Scranton, M. I., Paulmier, A., and van der Plas, A. K.: The role of open ocean boundary forcing on seasonal to decadal-scale variability and long-term change of natural shelf hypoxia, Environmental Research Letters, 6, 025002, 10.1088/1748-9326/6/2/025002, 2011.

Monteiro, P. M. S., Nelson, G., van der Plas, A., Mabille, E., Bailey, G. W., and Klingelhoeffer, E.: Internal tide—shelf topography interactions as a forcing factor governing the large-scale distribution and burial fluxes of particulate organic matter (POM) in the Benguela upwelling system, Continental Shelf Research, 25, 1864-1876, https://doi.org/10.1016/j.csr.2005.06.012, 2005.

Monteiro, P. M. S., van der Plas, A., Mohrholz, V., Mabille, E., Pascall, A., and Joubert, W.: Variability of natural hypoxia and methane in a coastal upwelling system: Oceanic physics or shelf biology?, Geophysical Research Letters, 33, doi:10.1029/2006GL026234, 022006, 2006.

Nagel, B., Gaye, B., Lahajnar, N., Struck, U., and Emeis, K.-C.: Effects of current regimes and oxygenation on particulate matter preservation on the Namibian shelf: Insights from amino acid biogeochemistry, Marine Chemistry, 186, 121-132, http://dx.doi.org/10.1016/j.marchem.2016.09.001, 2016.

Nagel, B., Emeis, K.-C., Flohr, A., Rixen, T., Schlarbaum, T., Mohrholz, V., and van der Plas, A.: N-cycling and balancing of the N-deficit generated in the oxygen minimum zone over the Namibian shelf—An isotope-based approach, Journal of Geophysical Research: Biogeosciences, 118, 361 - 371, 10.1002/jgrg.20040, 2013.

Nowicki, M., DeVries, T., and Siegel, D. A.: Quantifying the Carbon Export and Sequestration Pathways of the Ocean's Biological Carbon Pump, Global Biogeochemical Cycles, 36, e2021GB007083, https://doi.org/10.1029/2021GB007083, 2022.

Ohde, T. and Dadou, I.: Seasonal and annual variability of coastal sulphur plumes in the northern Benguela upwelling system, PLOS ONE, 13, e0192140, 10.1371/journal.pone.0192140, 2018.

Ohde, T., Siegel, H., Reißmann, J., and Gerth, M.: Identification and investigation of sulphur plumes along the Namibian coast using the MERIS sensor, Continental Shelf Research, 27, 744-756, 2007.

Paropkari, A. L., Babu, C. P., and Mascarenhas, A.: New evidence for enhanced preservation of organic carbon in contact with oxygen minimum zone on the western continental slope of India, Marine Geology, 111, 7-13, 1993.

Passow, U. and Carlson, C. A.: The biological pump in a high CO2 world, Marine Ecology Progress Series, 470, 249-271, 2012.

Pauly, D. and Christensen, V.: Primary production required to sustain global fisheries, Nature, 374, 255-257, 1995.

Pendleton, L., Donato, D. C., Murray, B. C., Crooks, S., Jenkins, W. A., Sifleet, S., Craft, C., Fourqurean, J. W., Kauffman, J. B., Marbà, N., Megonigal, P., Pidgeon, E., Herr, D., Gordon, D., and Baldera, A.: Estimating Global "Blue Carbon" Emissions from Conversion and Degradation of Vegetated Coastal Ecosystems, PLOS ONE, 7, e43542, 10.1371/journal.pone.0043542, 2012.

Pitcher, G. C. and Probyn, T. A.: Anoxia in southern Benguela during the autumn of 2009 and its linkage to a bloom of the dinoflagellate Ceratium balechii, Harmful Algae, 11, 23-32, https://doi.org/10.1016/j.hal.2011.07.001, 2011.

Pitcher, G. C., Probyn, T. A., du Randt, A., Lucas, A. J., Bernard, S., Evers-King, H., Lamont, T., and Hutchings, L.: Dynamics of oxygen depletion in the nearshore of a coastal embayment of the southern Benguela upwelling system, Journal of Geophysical Research: Oceans, 119, 2183-2200, https://doi.org/10.1002/2013JC009443, 2014.

Reynolds, B., Rayner, N. A., Smith, T. M., Stokes, D. C., and Wang, W.: An improved insitu and satellite SST analysis for climate, Journal of Climate, 15, 1609 - 1625, 2002.

Riebesell, U., Schulz, K. G., Bellerby, R. G. J., Botros, M., Fritsche, P., Meyerhofer, M., Neill, C., Nondal, G., Oschlies, A., Wohlers, J., and Zollner, E.: Enhanced biological carbon consumption in a high CO_2 ocean, Nature, 450, 545-548, 2007.

Rixen, T.: Past changes in and present status of the coastal carbon cycle, Cambridge Prisms: Coastal Futures, 1-35, 10.1017/cft.2023.20, 2023.

Rixen, T., Haake, B., Ittekkot, V., Guptha, M. V. S., Nair, R. R., and Schlüssel, P.: Coupling between SW monsoon-related surface and deep ocean processes as discerned from continuous particle flux meausurements and correlated satellite data, Journal of Geophysical Research, 101, 28,569-528,582, 1996.

Rixen, T., Cowie, G., Gaye, B., Goes, J., do Rosário Gomes, H., Hood, R. R., Lachkar, Z., Schmidt, H., Segschneider, J., and Singh, A.: Reviews and syntheses: Present, past, and future of the oxygen minimum zone in the northern Indian Ocean, Biogeosciences, 17, 6051-6080, 10.5194/bg-17-6051-2020, 2020.

Rixen, T., Lahajnar, N., Lamont, T., Koppelmann, R., Martin, B., van Beusekom, J. E. E., Siddiqui, C., Pillay, K., and Meiritz, L.: Oxygen and Nutrient Trapping in the Southern Benguela Upwelling System, Frontiers in Marine Science, 8, 1367, 2021a.

Rixen, T., Borowski, P., Duncan, S., Heinatz, K., Hirschmann, S., Horton, M., Hüge, F., Janßen, S., Jordan, T., Kaufmann, M., Kremer, K., Labis, E., Martin, B., Mayer, B., Meiritz, L., Paulus, E., Pinter, S., Plewka, J., Reule, N., Rommel, A., Schneider, T., Siddiqui, C., Springer, B., Stanbro, K., Stegeman, H., Wallschuss, S., Welsch, A., Wenzel, J., Witting, K., and Zankl, S.: Trophic Transfer Efficiency in the Benguela Current, Cruise No. SO285, August 20th - November 2nd 2021, Emden (Germany) - Emden (Germany), Gutachterpanel Forschungsschiffe;, Bonn2510-764X, 1-128, 10.48433/cr_so285, 2021b.

Rixen, T., Lahajnar, N., Lamont, T., Koppelmann, R., Martin, B., Meiritz, L., Siddiqui, C., van der Plas, A.K.: Chapter 25 - The Marine Carbon Footprint: Challenges in the Quantification of the CO_2 Uptake by the Biological Carbon Pump in the Benguela Upwelling System, in: Sustainability of Southern African Ecosystems under Global Change, edited by: von Maltitz,, G.P., Midgley, G.F., Veitch, J., Brümmer, C., Rötter, R.P., Viehberg, F.A. and Veste, M., Springer Ecological Studies 248, 729-757, ISBN 978-3-031-10947-8, https://doi.org/10.1007/978-3-031-10948-5, 2024.

Rubio, A., Blanke, B., Speich, S., Grima, N., and Roy, C.: Mesoscale eddy activity in the southern Benguela upwelling system from satellite altimetry and model data, Progress in Oceanography, 83, 288-295, https://doi.org/10.1016/j.pocean.2009.07.029, 2009.

Sell, A.F., von Maltitz, G.P., Auel, H., Biastoch, A., Bode-Dalby, M., Brandt, P., Duncan, S.E., Ekau, W., Fock, H.O., Hagen, W., Huggett, J.A., Koppelmann, R., Körner, M., Lahajnar, N., Martin, B., Midgley, G.F., Rixen, T., van der Lingen, C.D., Verheye, H.M., Wilhelm, M.R.: Chapter 2 - Unique Southern African Terrestrial and Oceanic Biomes and Their Relation to Steep Environmental Gradients, in: Sustainability of Southern African Ecosystems under Global Change, edited by: von Maltitz,, G.P., Midgley, G.F., Veitch, J., Brümmer, C., Rötter, R.P., Viehberg, F.A. and Veste, M., Springer Ecological Studies 248, 23-88, ISBN 978-3-031-10947-8, https://doi.org/10.1007/978-3-031-10948-5, 2024.

Shannon, L. V. and Nelson, G.: The Benguela: Large Scale Features and Processes and System Variability, in: The South Atlantic: Present and Past Circulation, edited by: Wefer, G., Berger, W. H., Siedler, G., and Webb, D. J., Springer Berlin Heidelberg, Berlin, Heidelberg, 163-210, 10.1007/978-3-642-80353-6_9, 1996.

Shannon, L. V. and O'Tool, M. J.: Sustainability of the Benguela: ex Africa semper aliquid novi, in: Large Marine Ecosystems of the World: Trends in Exploitation, Protection and Research, edited by: Hempel, G., and Sherman, K., Elsevier Science, Amsterdam, The Netherlands, 227 - 253, 2003.

Shillington, F. A., Reason, C. J. C., Duncombe Rae, C. M., Florenchie, P., and Penven, P.: Large scale physical variability of the Benguela Current Large Marine Ecosystem (BCLME), in: Benguela: Predicting a large marine ecosystem, edited by: Shannon, L. J., Hempel, G., Malanotte-Rizzoli, P., Moloney, C. L., and Woods, J., Elsevier, Amsterdam, 49 - 70, 2006.

Siddiqui, C., Rixen, T., Lahajnar, N., Van der Plas, A. K., Louw, D. C., Lamont, T., and Pillay, K.: Regional and global impact of CO_2 uptake in the Benguela Upwelling System through preformed nutrients, Nature Communications, 14, 10.1038/s41467-023-38208-y, 2023.

Smetacek, V., Brockel, K. V., Zeitzschel, B., and Zenk, W.: Sedimentation of particulate matter during a phytoplankton spring bloom in relation to hydrographical regime, Marine Biology, 47, 211-226, 10.1007/bf00541000, 1978.

Steinberg, D. K. and Landry, M. R.: Zooplankton and the Ocean Carbon Cycle, Annual Review of Marine Science, 9, 413-444, 10.1146/annurev-marine-010814-015924, 2017.

Stramma, L., Johnson, G. C., Sprintall, J., and Mohrholz, V.: Expanding oxygen-minimum zones in the tropical oceans, Science, 320, 655-658, 10.1126/science.1153847, 2008.

Stramma, L., Prince, E. D., Schmidtko, S., Luo, J., Hoolihan, J. P., Visbeck, M., Wallace, D. W. R., Brandt, P., and Kortzinger, A.: Expansion of oxygen minimum zones may reduce available habitat for tropical pelagic fishes, Nature Clim. Change, 2, 33-37, http://www.nature.com/nclimate/journal/v2/n1/abs/nclimate1304.html#supplementary-information, 2012.

Stukel, M. R., Irving, J. P., Kelly, T. B., Ohman, M. D., Fender, C. K., and Yingling, N.: Carbon sequestration by multiple biological pump pathways in a coastal upwelling biome, Nature Communications, 14, 2024, 10.1038/s41467-023-37771-8, 2023.

Sydeman, W. J., García-Reyes, M., Schoeman, D. S., Rykaczewski, R. R., Thompson, S. A., Black, B. A., and Bograd, S. J.: Climate change and wind intensification in coastal upwelling ecosystems, Science, 345, 77, 2014.

Turner, J. T.: Zooplankton fecal pellets, marine snow, phytodetritus and the ocean's biological pump, Progress in Oceanography, 130, 205-248, http://dx.doi.org/10.1016/j.pocean.2014.08.005, 2015.

Tutasi, P. and Escribano, R.: Zooplankton diel vertical migration and downward C flux into the oxygen minimum zone in the highly productive upwelling region off northern Chile, Biogeosciences, 17, 455-473, 10.5194/bg-17-455-2020, 2020.

van der Plas, A. K., Monteiro, P. M. S., and Pascall, A.: Cross-shelf biogeochemical characteristics of sediments in the central Benguela and their relationship to overlying water column hypoxia, African Journal of Marine Science, 29, 37-47, 10.2989/AJMS.2007.29.1.3.68, 2007.

von Maltitz, G.P., Midgley, G.F., Veitch, J., Brümmer, C., Rötter, R.P., Rixen, T., Brandt, P., Veste, M.: Chapter 32 - Synthesis and Outlook on Future Research and Scientific Education in Southern Africa, in: Sustainability of Southern African Ecosystems under Global Change, edited by: von Maltitz,, G.P., Midgley, G.F., Veitch, J., Brümmer, C., Rötter, R.P., Viehberg, F.A. and Veste, M., Springer Ecological Studies 248, 933-964, ISBN 978-3-031-10947-8, https://doi.org/10.1007/978-3-031-10948-5, 2024.

Veitch, J., Penven, P., and Shillington, F.: The Benguela: A laboratory for comparative modeling studies, Progress in Oceanography, 83, 296-302, https://doi.org/10.1016/j.pocean.2009.07.008, 2009.

Verheye, H. M., Lamont, T., Huggett, J. A., Kreiner, A., and Hampton, I.: Plankton productivity of the Benguela Current Large Marine Ecosystem (BCLME), Environmental Development, 17, 75-92, https://doi.org/10.1016/j.envdev.2015.07.011, 2016.

Vorrath, M.-E., Lahajnar, N., Fischer, G., Libuku, V. M., Schmidt, M., and Emeis, K.-C.: Spatiotemporal variation of vertical particle fluxes and modelled chlorophyll a standing stocks in the Benguela Upwelling System, Journal of Marine Systems, 180, 59-75, https://doi.org/10.1016/j.jmarsys.2017.12.002, 2018.

Weldrick, C. K., Makabe, R., Mizobata, K., Moteki, M., Odate, T., Takao, S., Trebilco, R., and Swadling, K. M.: The use of swimmers from sediment traps to measure summer community structure of Southern Ocean pteropods, Polar Biology, 44, 457-472, 10.1007/s00300-021-02809-4, 2021.

26

Figure Caption

Figure 11 POC concentration of surface sediment samples in the BUS from various research expeditions published in Emeis et al. (2018). Yellow stars show deployment drifter positions; red diamonds show long-term mooring locations. Contour lines in 1.5 % steps. Red dashed areas indicate the nBUS and sBUS, respectively (Hutchings et al., 2009).

Figure 12 Oxygen concentrations along a transect in the nBUS and sBUS during cruise SO285, showing the near-bottom OMZ in the nBUS (a) and sBUS (b), and the OMZ on the continental slope in the nBUS. Oxygen data (unpublished) from CTD casts conducted during cruise SO285.

Figure 13 Monthly mean annual cycles of sea surface temperatures (SST, a) and primary production rates (PP, b) in the nBUS and sBUS area, respectively. Satellite data (OI SST, and PP) have been downloaded in November 2023 (see method section). Dotted areas indicate the sampling periods of SO283 and SO285 cruises, respectively. Error bars indicate the standard deviation of PP and SST within the time period 1981-2023.

Figure 4 Primary production rates (SeaWiFS) in mg C m^{-2} day^{-1} during the research cruises M153, SO283 and SO285 as well as the locations of the drifters deployments (black numbers) and long-term sediment trap mooring sites (white circles).

Figure 5 Proportion of zooplankton groups in the active POC averaged over all traps with a mean standard deviation of 15±8%. Amph- amphipods, Cope- copepods, Deca – decapoda, Euph- euphausiids, Ostr- ostracodes, Ptero- pteropods, Fish- fish larvae, Gela – gelatinous organisms, Zoo- zooplankton not further identified.

Figure 6 POC flux rates measured off Walvis Bay in the nBUS and Hondeklip Bay in the sBUS(a) and the mean annual cycle (b) derived from the data shown in (a).

Figure 14 Active (a) and passive POC flux (b) averaged over all traps deployed at the same water depth versus water depth, including mean passive POC flux rates (squares) of the long-term moorings in the nBUS and sBUS.

Figure 15 Mean POC flux rates (red and blue dots) versus water depths of 0 m - 2500 m (a) and 0 m - 500 m (b). The curves are Martin curves with a 'b' of -0.74 (black) and -0.86 (grey). The result of an nBUS trap at 10 m water depth (see b, red circle at 10 m depth) was not considered in the curve fitting. Sediment trap data (black dots) taken from Vorrath et al. (2018); squares depict the mean POC flux of the long-term moorings from this study.

Figure 16 Temperature profiles at the CTD stations (depth resolution of 1 m) closest to the long-term mooring site during the cruises SO285 austral spring (a) and M153 austral summer (b). The positions of the mooring stations are shown in Fig. 1 and Tab.1. Decimal places indicate that there have been several casts at the stations. Station 7 was a long station at which five CTD casts have been carried out over the course of a day. It should be noted that the MLD showed a diurnal variation, with a maximum depth of approx. 14 meters. A maximum MLD of approx. 14 m was also shown in the nBUS (station 32). During the SO285 cruise in austral spring, the MLDs varied between approx. 30 m and 15 m. The dashed lines were inserted to illustrate the maximum MLDs. CTD data available at https://www.pangaea.de.

Figure 10 System schematics in the nBUS (a) and the sBUS (b). Green arrows and their size characterize the active transport pathways. The black curve shows the Martin curve based passive POC flux which is similar in both systems. Red and blue arrows show the contribution and entering of upwelling source water masses. The brown areas indicate POC-rich mud belt in the BUS which is absent in sBUS.

Table Caption

Table 1 Overview of moored sediment trap deployments.

Table 2 Overview of drifter deployments.

Table 3 List of drifter-related cruises.